ISSN 1330-3651(Print), ISSN 1848-6339 (Online)
Received: 21 November 2025; Accepted: 23 January 2026
https://doi.org/10.17559/TV-20251121003148
Original scientific paper

Transfer Entropy-Based Research on Vibration Source Tracing and Key Paths in a Hydropower House

Baoping ZHI, Mengran CHENG, Jingjing QIN*, Zihan SONG

Abstract: The vibration sources of power house of hydroelectric power station are complex, and are prone to undesirable vibrations. Among them, the transfer path of hydraulic vibration is an important part of vibration control and operation monitoring. Accurately separating hydraulic vibration sources is crucial to identify the transfer path. To accurately identify the transfer path of the hydraulic vibration source in the structure of the power house of hydroelectric power station, a method combining CEEMDAN-SVD and TE is proposed. The rationality is verified through cross-correlation simulation signals, which are applied to the analysis of the vibration transfer path of the power house of hydroelectric power station. Firstly, based on the vibration test data, CEEMDAN-SVD is used to adaptively perform eigenvector decomposition by the signal energy. Secondly, based on the decomposed vibration signals, the TE (Transfer Entropy) is utilized to identify and analyze the transfer paths of partial vibration source of hydroelectric power station structure. Finally, the applicability of this method to the vibration transfer path of the factory building structure was verified by the quantitative index - information transmission rate. Research shows that the main transfer path of the vibration caused by the vortex rope is as follows: draft tube → undercarriage or stator base → upper floor structure of the power house. The research results are significant for the vibration control and operation monitoring of hydropower station, which provide new ideas for vibration analysis in the engineering field.

Keywords: power house of hydroelectric power station; TE; transfer path; vibration response; vortex rope

1 INTRODUCTION

Currently, as our country's installed capacity and input head of hydropower stations expand, vibration difficulties in powerhouse structures caused by a variety of reasons are growing more severe. The vibration source of a hydroelectric power station consists of three major components: mechanical, electromagnetic, and hydraulic. As the primary energy source, the investigation and research of hydraulic vibration sources is critical. During the unit's transitional operation, major hydraulic instability problems are likely to emerge, which might generate resonance in the factory building and be exceedingly unfavorable for operation. The swing's low-frequency vibration is mostly caused by the vortex rope, which works on the draft tube, roof cover, revolver, spiral case, and other structures. The vortex rope operates on the draft tube, roof cover, revolver, spiral case, and other structures, and it is the primary cause of low-frequency vibration in the turbine's swing and rotational components, as well as the draft tube wall. Accurately identifying the vibration range of the vortex rope, as well as analyzing the causes of sudden changes in its vibration transfer path and the amount of transmitted information is critical for the operation monitoring and vibration control of the power house of a hydroelectric power station.

Vibration transfer route analysis entails creating input-output models for the system under consideration, which is increasingly commonly used in industries like autos and shipping. Wang Haijun [1, 2] used the structural sound intensity technique to study and analyze the vibration transmission law from the overflow dam to the interior of the main plant, resulting in a design foundation for minimizing transmission. Xu Wei [3] did a study on the vibration characteristics of pumped storage power station structures by power flow theory and the energy technique. Qin Liang [4-6] analyzed and studied the energy proportion based on the frequency division of vibration signals. [7] studied the contact relationship between spiral case and concrete and the vibration transmission mechanism of pumped storage power stations by using boundary contact. Wei Peng [8] analyzed the vibration response characteristics of the power house of hydroelectric power station structure by using the vibration signals of the building structure.

The above-mentioned scholars have conducted a series of studies on the vibration characteristics of power house of hydroelectric power station, but there are relatively few analyses of the transfer paths of hydraulic vibration sources within the structure. However, accurately analyzing the transfer paths of hydraulic vibration sources is significant for vibration control. A hydropower station is a complex coupled system of "water - electromechanical - power plant", with complex vibration signal sources and strong noise. To make the analysis of the transfer path of the hydraulic vibration source more accurate, it is also crucial to separate and reduce the noise of the original signal. This paper proposes a new algorithm combining CEEMDAN-SVD (Complete Ensemble Empirical Mode Decomposition with Adaptive Noise-Singular Value Decomposition) and TE (abbreviated as TE) to analyze the vibration transfer path of the power house of hydroelectric power station structure. Based on CEEMDAN-SVD, the noise reduction decomposition of the original signal is carried out to obtain the hydraulic vibration signal (vortex rope). The vibration transfer path caused by the hydraulic vibration source and vortex rope is identified by the TE, and its vibration characteristics and transmission laws are analyzed, providing a new idea for the vibration control of the hydraulic vibration source and the analysis of vibration characteristics with the aim of reducing the accident rate of hydropower station plants caused by undesirable vibrations.

2 BASIC THEORY

TE is a concept in information theory and dynamic systems that quantifies the influence of one time series on the future values of another time series or information transfer. It was proposed by scholar Thomas Schreiber in 2000 [9]. TE quantifies the directed, time-asymmetric flow

of information between two dynamic systems or stochastic processes, capturing both the direction of signal propagation and the degree of energy coupling. Owing to its inherent asymmetry, high sensitivity, and freedom from specific distributional or model assumptions, TE has become a standard metric for dissecting causal relationships and information transfer in complex systems. Applications now span biology, economics, and communications engineering [10, 11].

According to Schreiber's definition of TE, the calculation of TE is based on Markov stochastic processes. Assuming the transition probability of y affecting x is p, then:

$$T_{y\to x}\left(x(1)\middle|\ x^{(k)},y^{(l)}(\tau)\right)=\int p\left(x(1),x^{(k)},y^{(l)}(\tau)\right)\log_2\left\{\frac{p\left(x(1)\middle|\ x^{(k)},y^{(l)}(\tau)\right)}{p\left(x(1)\middle|\ x^{(k)}\right)}\right\}\times \mathrm{d}x(1)\mathrm{d}x^{(k)}\mathrm{d}y^{(l)} \tag{1}$$

In the formula, k and l are respectively the order of the Markov random process x and y, and $T_{y\to x}$ is the TE of the dynamic process y to x.

$T_{y\to x}$ quantifies the influence degree of time series on each other, that is, the influence degree of y on x. When the future of x is not affected by the state y, there is no energy transfer between the two signals, and the TE value is 0, that is, $TE=0$. When $T_{y\to x}\neq T_{x\to y}$, it indicates that there is an asymmetry in the amount of information between x and y, that is, the signal has a direction during the process of energy transmission. When $T_{y\to x}>T_{x\to y}$, it shows that the process of information transmission is $y\to x$.

TE requires the probability distribution calculation of various states and the high-dimensional probability density function, which is rather complex. To simplify the calculation process and without affecting the calculation results, it is assumed that both the dynamic process x and y are of the first order, that is, $k=l=1$. When $k=l=1$, the calculation efficiency based on TE has been greatly improved [12 - 13].

For dynamic processes x and y, TE simplifies to the product of variance and covariance [14]:

$$T_{y\to x}\left(x(1)\middle|\ x,y(\tau)\right)=\frac{1}{2}\log_2\left(\frac{\left|D_{x(1),x,y(\tau)}\right\|\ D_x\right|}{\left|D_{x,y(\tau)}\right\|\ D_{x(1),x}\right|}\right) \tag{2}$$

In the formula, "||"represents finding the determinant of a matrix.

$$D_{x(1),x,y(x)}=\begin{bmatrix}E\left[x(n+1)x(n+1)\right] & E\left[x(n)x(n+1)\right] & E\left[y(n+\tau)x(n+1)\right]\\ E\left[x(n)x(n+1)\right] & E\left[x(n)x(n)\right] & E\left[x(n)y(n+\tau)\right]\\ E\left[y(n+\tau)x(n+1)\right] & E\left[y(n+\tau)x(n)\right] & E\left[y(n+\tau)x(n+\tau)\right]\end{bmatrix} \tag{3}$$

$$D_x=E\left[x(n)x(n)\right]=\sigma_x^2 \tag{4}$$

$$D_{x,y(\tau)}=\begin{bmatrix}E\left[x(n)x(n)\right] & E\left[x(n)y(n+\tau)\right]\\ E\left[y(n+\tau)x(n)\right] & E\left[y(n+\tau)x((n+\tau)\right]\end{bmatrix} \tag{5}$$

$$D_{x(1),x}=\begin{bmatrix}E\left[x(n+1)x(n+1)\right] & E\left[x(n)x(n+1)\right]\\ E\left[x((n+1)x(n)\right]\end{bmatrix}\quad E\left[x(n)x(n)\right] \tag{6}$$

In the formula, E[] represents expectation, σ means standard deviation. D represents variance. τ is time delay, and n is time series.

Based on the dynamic process and the assumption that both are first-order, cross-correlation and autocorrelation functions are introduced.

Cross-correlation function is as follows.

$$R_{xy}(\tau)=E\left[x(n)y(n+\tau)\right] \tag{7}$$

Autocorrelation function is shown as follows.

$$R_{xx}(\tau)=E\left[x(n)x(n+\tau)\right] \tag{8}$$

To enhance the performance of the TE algorithm and improve its generalization ability, normalization processing is carried out on it.

Normalized autocorrelation function is as follows.

$$\hat{R}_{xx}(\tau)=\frac{R_{xx}(\tau)}{R_{xx}(0)} \tag{9}$$

$$\rho_{xy}(\tau)=\frac{R_{xy}(\tau)}{\sqrt{R_{xx}(0)R_{yy}(0)}} \tag{10}$$

Normalize the correlation functions at different scales as shown in Eq. (11):

$$T_{y\to x}\left(x(1)\middle|\ x,y(\tau)\right)=\frac{1}{2}\log_2\left\{\frac{\left(\rho_{xy}^2(\tau)-1\right)\left(\hat{R}_{xx}(1)-1\right)}{2\rho_{xy}(\tau-1)\hat{R}_{xx}(1)\rho_{xy}(\tau)-\rho_{xy}^2(\tau-1)-\hat{R}_{xx}(1)-\rho_{xy}^2(\tau)+1}\right\} \tag{11}$$

In the formula, $\rho_{xy}(\tau)$ is the cross-correlation function of x and y, and $\hat{R}_{xx}(\tau)$ is the autocorrelation function of x.

3 SIMULATION VERIFICATION

Two sets of vibration simulation signals A and B were constructed to verify the correctness and applicability of TE in identifying the transmission of vibration signals. The relationship between A and B is characterized by their correlation coefficient μ (when $\mu=0$, A and B are two independent signals). By changing the correlation coefficient between A and B, the sensitivity of the TE value to the signal transmission direction is verified. Since the vibration signals collected in practical engineering applications are accompanied by various noises, white noise is added to the simulation signal to analyze the influence of noise on the TE value. The constructed simulation signals A and B are as follows:

$$A=\cos\left(2\pi x_1 t\right)+0.2\sin\left(2\pi x_2 t\right) \tag{12}$$

$$B=\mu A+0.1\cos\left(2\pi x_1 t\right)\cos\left(2\pi x_2 t\right)-\cos\left(2\pi x_2 t\right) \tag{13}$$

In the formula, $x_1=40$, $x_2=4$; μ is used for the degree of correlation.

By changing the relevant parameter μ, the applicability and sensitivity of ITE in identifying signal direction and correlation are verified. When both ITE are 0, it indicates that there is no energy transfer between A and B, and the two signals are independent of each other.

3.1 The Influence of Correlation on the Value of TE

The correlation coefficients between the two sets of simulation signals A and B are $\mu=0.2$, $\mu=0.4$, $\mu=0.6$ and $\mu=0.8$. This paper calculates the TE values $TE_{A\to B}$ and $TE_{B\to A}$ under different correlation coefficients respectively. The variation curve of the TE value with time is shown in Fig. 1.

As can be seen from Fig. 1: (1) The transmission direction between signals can be accurately determined based on the TE value. When $\mu=0.2$, $\mu=0.4$, $\mu=0.6$ and $\mu=0.8$ at any time period, $TE_{B\to A}$ is less than $TE_{A\to B}$. It indicates that the information transmission direction between signals A and B is $A\to B$, which is consistent with the known signal flow direction. This proves that the TE algorithm to determine the information transmission law between different signals is effective. (2) The TE algorithm has a high sensitivity in identifying the direction of signal transmission. When the correlation coefficient between simulation signals A and B is reached by $\mu=0.8$, the corresponding TE value is relatively large, with the maximum reaching 1.4, and the direction of information transmission is $A\to B$. When the correlation coefficient between simulation signals A and B is low, the corresponding TE is relatively small, with the maximum value being only 0.6. However, the transfer path remains clear, and the transmission direction is $A\to B$. When the correlation between the two signals is low, the transmission direction between the signals can still be accurately determined, indicating that the sensitivity of TE in discriminating the direction of information transmission is high. (3) The magnitude of the TE value reflects to A certain extent the degree of correlation between signals A and B. As the correlation coefficients of the two groups of simulation signals continue to increase, TE also increases, especially when the period is between 0.04 and 0.05, which is consistent with the magnitude of the correlation coefficient of the constructed signal, indicating that the TE value can reflect the correlation degree between the two signals to a certain extent.

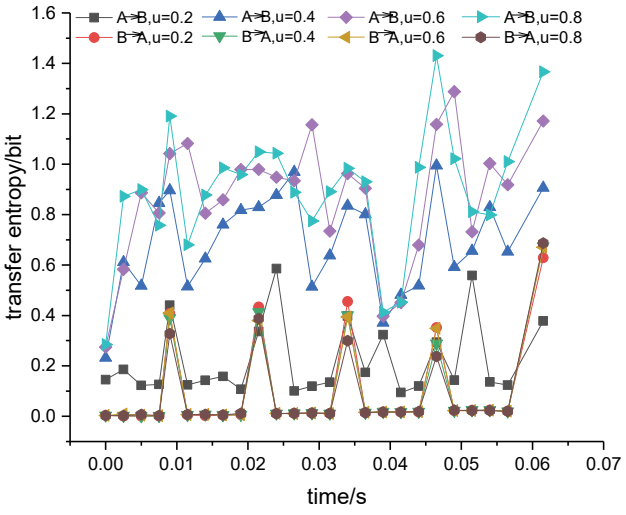

Figure 1 TE curve

3.2 The Influence of Noise on the Value of TE

For two sets of constructed simulation signals A and B, the influence of noise on the TE was studied by the control variable method. The correlation coefficients between the signals were respectively $\mu=0.2$, $\mu=0.4$, $\mu=0.6$, and $\mu=0.8$. When the same set of noise signals was added, the TE variation curves of the noisy signal and the pure signal were shown in Fig. 2.

It can be seen from Fig. 2 that: (1) Noise will have an impact on the probability distribution of information flow. When $\mu=0.2$, $\mu=0.4$, $\mu=0.6$ and $\mu=0.8$, comparing the pure signal with the noisy signal, it was found that the TE value of the noisy signal was greater than that of the pure signal. As it increases, the TE value of the noisy signal will also increase.

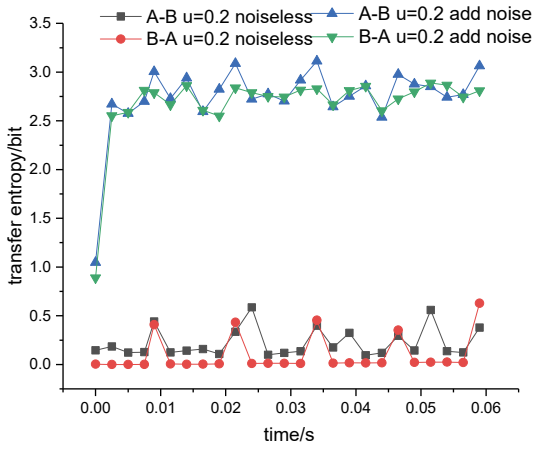

(a) The TE change curve of μ=0.2

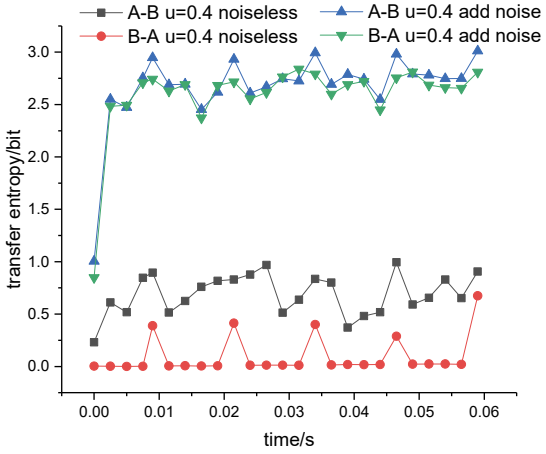

(b) The TE change curve of μ=0.4

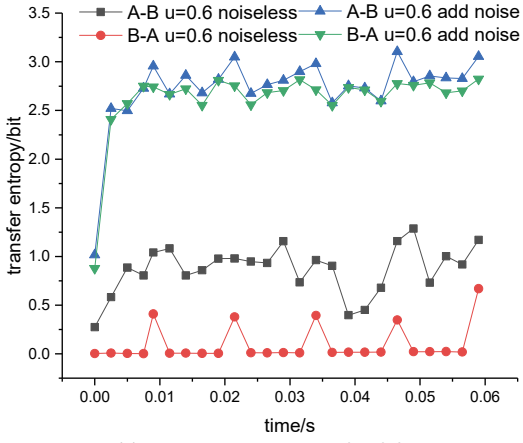

(c) The TE change curve of μ=0.6

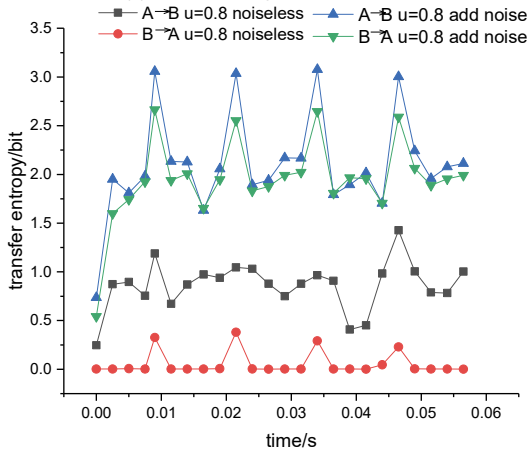

(d) the TE change curve of μ=0.8

Figure 2 TE curve

These indicate that the noisy signal will have a certain degree of influence on the probability distribution of the information flow. (2) The correlation degree is greater, and the variation range of TE is greater in the noisy signal. When the correlation coefficients are different, the variation range of the TE curve is different. When μ is 0.8, the variation range of the TE value is the largest. When μ is 0.2, the TE value changes the most. (3) The TE algorithm has certain anti-noise performance. Although the TE value of the noisy signal is greater than that of the pure signal, the direction of information transfer between signals A and B remains unchanged, indicating that noise affects the magnitude of the TE value. However, within a certain range, the noise signal does not change the direction of information transmission, and the TE algorithm has certain anti-noise performance.

4 ANALYSIS OF THE TRANSFER PATH OF THE POWER HOUSE OF HYDROELECTRIC POWER STATION

4.1 Project Overview

This research examines the Quxue Hydropower Station, situated on the Shuoqu River, a secondary tributary of the Jinsha River. The facility is characterized by a mixed development design, comprising underground powerhouses, water retention, and water conveyance structures. The station operates with a maximum water head of 210.3 meters and a minimum water head of 147.4 meters. The principal dynamic loads inducing vertical vibrations in both the powerhouse and the generating units originate from pressure pulsations associated with the vortex rope and the roof cover. Within the turbine unit's flow channel, the upward propagation of low-frequency vortex rope pulsations generates pressure fluctuations of corresponding frequency on the roof cover. Consequently, accelerometers installed on the generator floor slab are employed to monitor the vibrational responses of the upper structural components of the power station building. To some extent, the roof cover can characterize the flow-induced vibration of the draft tube. The measurement points of the stator and undercarriage foundation characterize the vibration at the machine pier position. Based on the above principles, four key parts, namely the roof cover, stator base, undercarriage foundation and generator floor, are selected to install acceleration sensors. The vibration test data was collected by the type vibration pickup of Dongfang Vibration Institute, and the type vibration pickup was used for verification. The test sensor is shown in Fig. 3. The corresponding relationship between the positions and numbers of the vibration measurement points collected is as follows: vibration measurement point 1- roof cover (*y* direction), vibration measurement point 2- undercarriage (*y* direction), vibration measurement point 3- stator (*y* direction), vibration measurement point 4- generator floor slab (*y* direction). The layout of the measurement points is shown in Fig. 4.

This paper analyzes the TE value of each measurement point of the hydropower station under three working conditions over time, which explores the magnitudes of TE values at each measurement point under different working conditions and the transfer path laws of hydraulic vibration at each measurement point (due to space limitations, only

the vibration transfer law of the vortex rope is listed). The vibration test conditions are shown in Tab. 1.

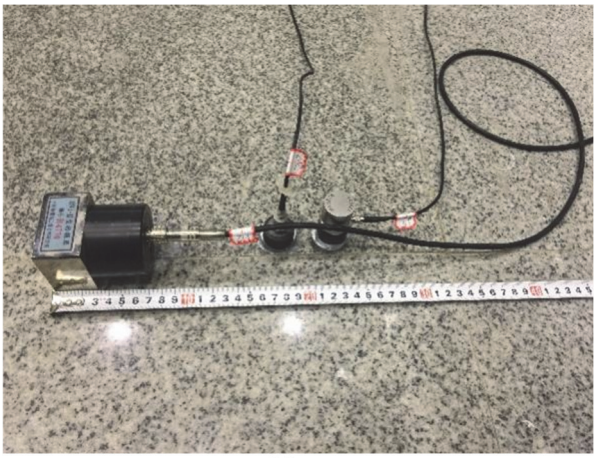

a) Sensor

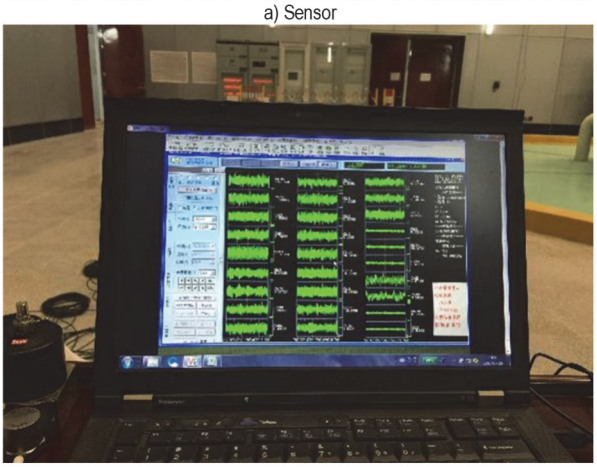

b) Information collection

Figure 3 Test sensor

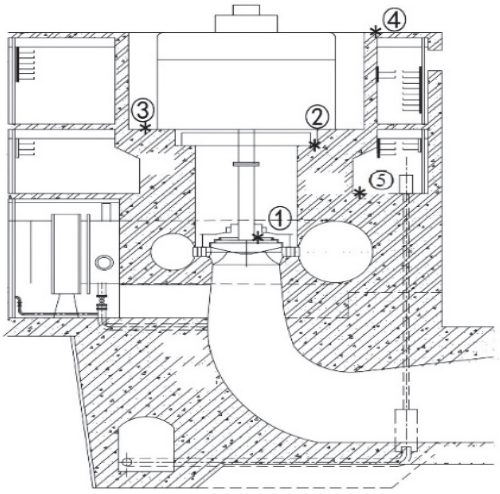

Figure 4 Layout of measurement points

Table 1 Vibration test conditions

Vibration testing conditions	Operation status of hydroelectric generator set	Sampling time / s	Sampling frequency / Hz
1	At the moment of starting the hydroelectric generator set	1000	1024
2	Stable operation of hydroelectric generator set	1000	1024
3	Instantaneous shutdown of hydroelectric generator set	1000	1024

4.2 Vibration Transfer Path Identification

Due to the complexity of the vibration sources in the power house of hydroelectric power station, the vibration signals are multi-source and have strong noise interference. Although TE has a certain anti-noise performance, the noise within a certain range will not affect the transmission direction of the signal. To make the calculation results more representative, before analyzing the vibration transfer path of the power house of hydroelectric power station, this paper introduces the CEEMDAN-SVD algorithm to preprocess the vibration measurement data and conduct vibration transfer path analysis on the target signal after data processing. The processing flow is as follows. The vibration transfer path identification and analysis flow are shown in Fig. 5.

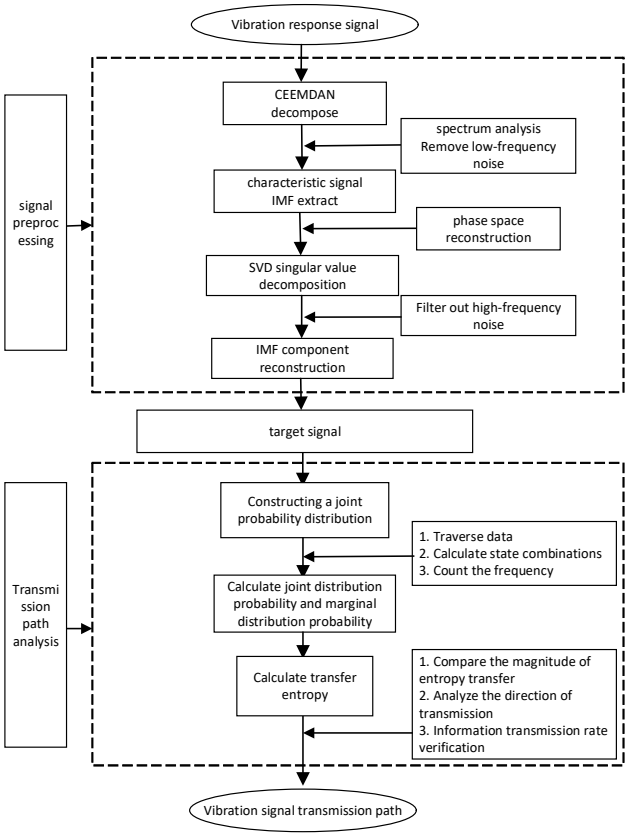

Figure 5 Flow chart of transfer path identification

(1) The acceleration sensor collects the vibration test signals corresponding to the set measurement points.

(2) Introduce CEEMDAN to screen out the IMF components that reflect the vibration characteristics of the structure.

(3) SVD filters out the high-frequency noise in the IMF component.

(4) Reconstruct the information of the IMF component and extract the target signal with characteristic information.

(5) Construct a joint probability distribution based on the target signal.

(6) Calculate the joint probability and marginal probability.

(7) Calculate the entropy value TE of the target signal varying with time.

(8) Draw the TE curves of each measurement point and analyze the transfer path of the vibration signal.

Vibration test data collection uses 891-II type vibration pickers, and verification is carried out with INV9828 type vibration pickers. To eliminate the influence of equipment, a low-pass filter is designed to remove noise below 0.20 Hz and power frequency noise. In this paper, the CEEMDAN-SVD technology is used to reduce noise, decompose and reconstruct the vibration measurement signal, which obtains the vortex rope vibration signal [16]. The vibration transmission path identification and analysis are carried out.

4.3 Transmission Path Analysis

The n_H =150 r/min of the hydroelectric generating unit of this hydropower station is 150, and the pulsation frequency of the vortex rope is calculated by the following empirical formula:

$$f = \left(\frac{n_H}{60}\right)\mu_s \tag{14}$$

In the formula, based on the statistics of some power stations in our country, the value μ_s is generally taken to μ_s=1/3 ~ 1/6. n_H represents the rated speed of the unit, with the unit r/min.

This paper takes the sum μ_s=1/3 and μ_s=1/6 respectively. Then: $f = (0.42 \sim 0.83)$ Hz, this calculated value is the corresponding frequency band range of the vibration caused by the vortex rope. The CEEMDAN-SVD algorithm is introduced to decompose the target signal within the corresponding frequency band range. Due to space limitations, only the vibration response spectrum and component time history diagram of the generator floor slab are provided, as shown in Figs. 6 and 7.

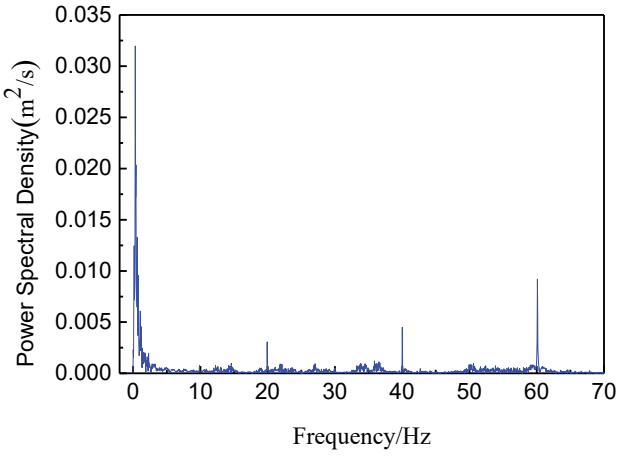

Figure 6 Frequency spectrum

CEEMDAN-SVD decomposition results in four IMF components, IMF1-IMF4 corresponding respectively to the four frequency bands in the vibration response spectrum analysis diagram. According to Eq. (3-1), the empirical vibration frequency range (0.42 ~ 0.83 Hz) of the vortex rope is calculated. The target signal is IMF4, which corresponds to the spectrum diagram, that is, the vibration response of the vortex rope is 0.5Hz. Based on the target signal decomposed by the CEEMDAN-SVD algorithm (the vibration signal of the pure vortex rope), the TE values of the vortex rope at each measurement point under different working conditions are calculated. Under vibration test condition 1 (the moment the hydropower station unit starts up), the vortex rope TE curve is shown in Fig. 8.

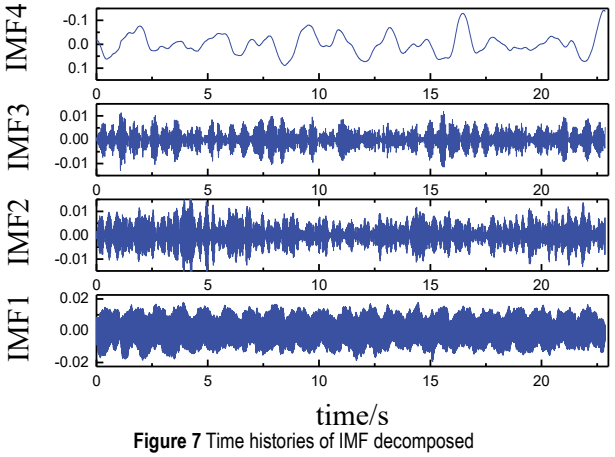

Figure 7 Time histories of IMF decomposed

From the comparative analysis in Figs. 8a-f, now when the hydroelectric generating unit of a hydropower station starts up, there are two vibration transfer paths caused by the vortex rope: Roof cover → undercarriage → Generator floor slab and Roof cover → Stator → Generator floor slab. From the characteristics of TE, it can be known that the magnitude of the TE value can represent the correlation degree between signals. The bidirectional entropy value is larger, the correlation degree is higher. The vibration signal with a larger TE value is the information source. In Fig. 8a, the transmission direction between the roof cover and the stator base is from the roof cover to the stator base. Similarly, by analyzing Figs. 8b, c, e, and f, it can be determined that the information transmission directions are respectively: from the roof cover to the generator floor slab, from the roof cover to the undercarriage, from the stator base to the generator floor slab, and from the undercarriage to the generator floor slab. In Fig. 8d, the TE curves of the stator base and the undercarriage almost coincide, and the TE value is much smaller than that of other measurement points. Therefore, the information transmission between the undercarriage and the stator base is ignored. 3. Under this test condition, in Figs. 8a, b, and e, $TE_{\text{roof cover}\rightarrow\text{generator floor slab}} < TE_{\text{roof cover}\rightarrow\text{stator base}}$ and $TE_{\text{stator base}\rightarrow\text{generator floor slab}} < TE_{\text{roof cover}\rightarrow\text{stator base}}$. The direction of vibration signal transmission caused by the vortex rope is Roof cover → Stator → Generator floor slab. Similarly, from the analysis of Figs. 8c, d, and f, it can be obtained that the vibration transfer path caused by another vortex rope is roof cover → undercarriage → Generator floor slab.

The TE variation curve of the vortex rope under vibration test condition 2 (stable operation of the hydropower station unit) is shown in Fig. 9.

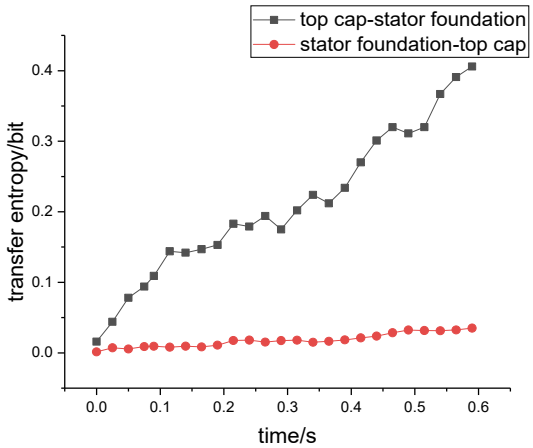

(a) TE curve of the roof cover and stator

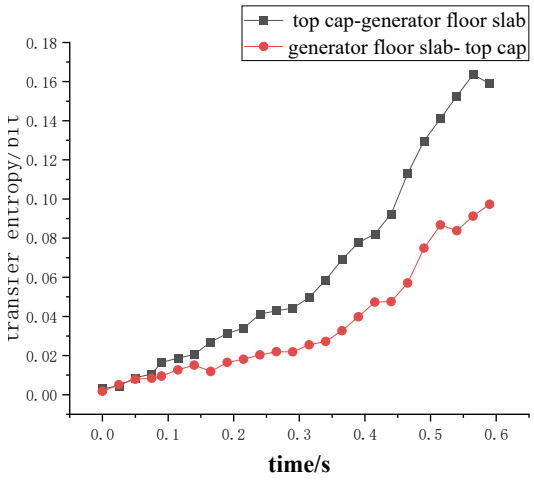

(b) TE curve of the roof cover and the floor slab of the generator

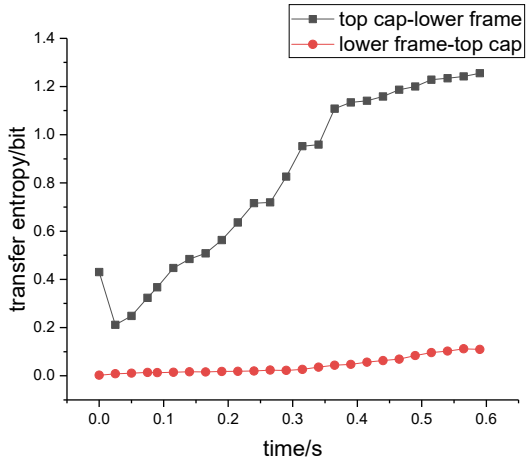

(c) TE curve of the roof cover and the undercarriage

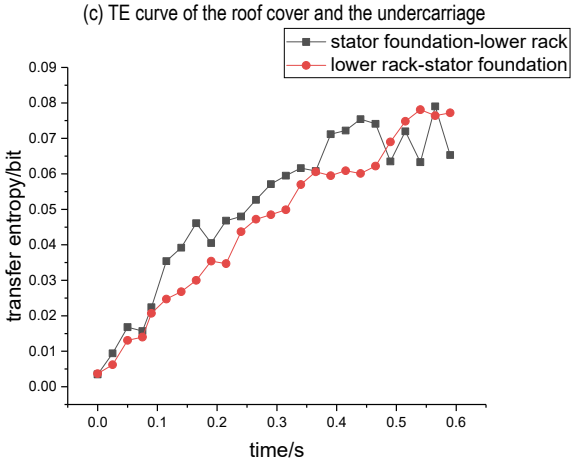

(d) TE curve of the stator base and the undercarriage

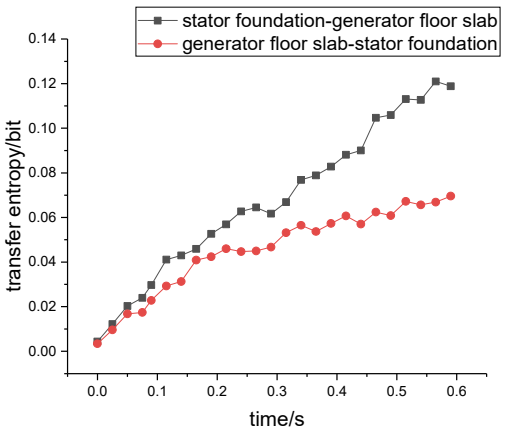

(e) TE curves of the stator and the generator floor slab

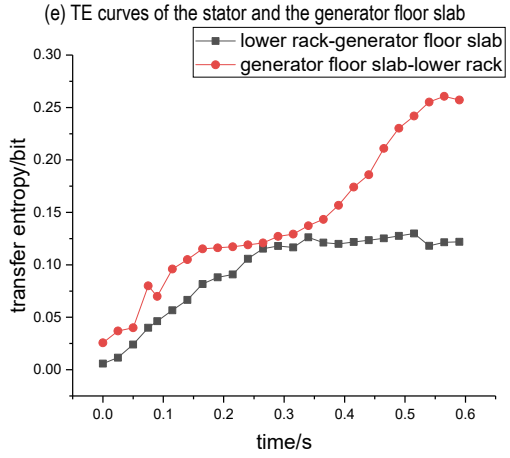

(f) TE curves of the undercarriage and the generator floor slab

Figure 8 TE curve of condition 1

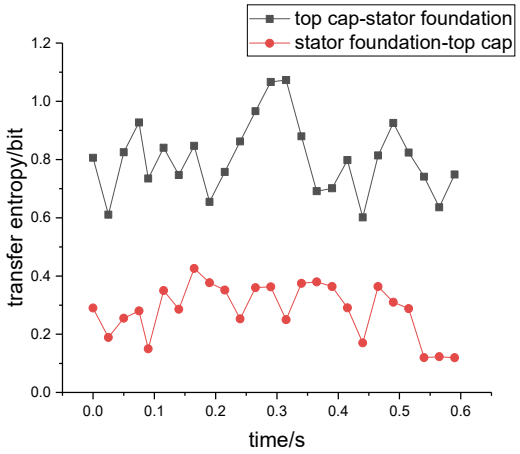

(a) TE curve of the stator base and the roof cover

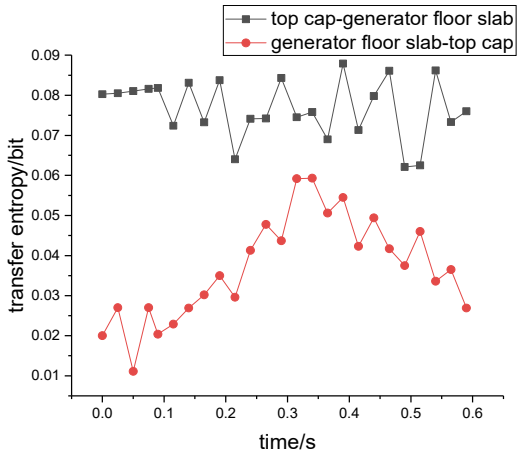

(b) TE curve of the generator floor slab and the roof cover

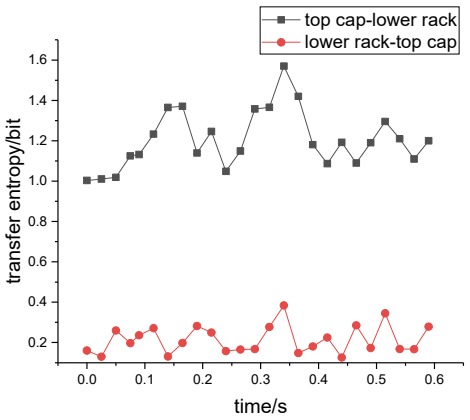

(c) TE curve of the undercarriage and the roof cover

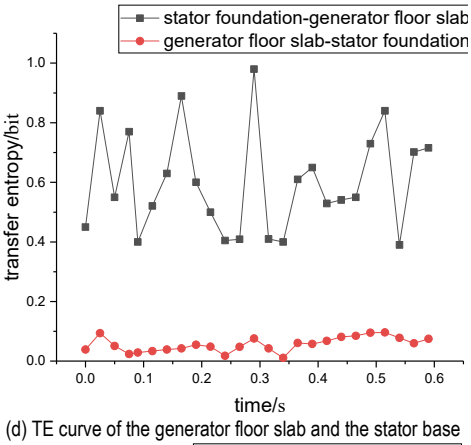

(d) TE curve of the generator floor slab and the stator base

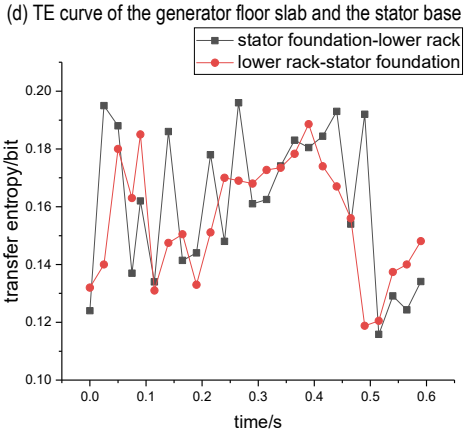

(e) TE curve of the undercarriage and stator base

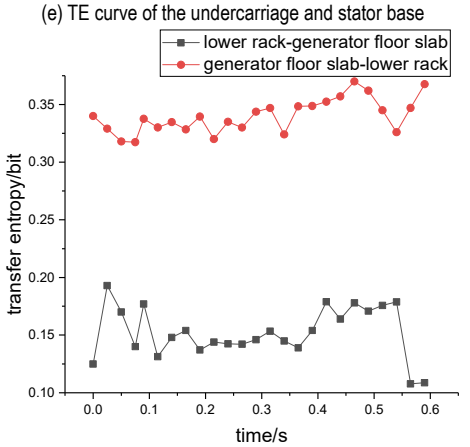

(f) TE curve of the generator floor slab and the undercarriage

Figure 9 TE curve of condition 2

By comparing Fig. 8 with Fig. 9, it can be concluded that: a) The TE algorithm can characterize the degree of correlation between two measurement points. The TE curve shows an upward trend now the unit is turned on. As the startup state gradually stabilizes, the TE value gradually increases. The TE curve tends to flatten under the stable operation of the unit. It indicates that as the unit starts up to stable operation (the water flowing through the hydroelectric generating unit changes from unstable to stable state), the correlation degree of the vibration caused by the vortex rope among the measurement points gradually increases. This conclusion is consistent with the actual operating status of the power house of hydroelectric power station. b) The TE value from the roof cover to the undercarriage is the largest, followed by that from the roof cover to the stator base, and the smallest from the roof cover to the generator floor slab. This indicates that the roof cover has the largest amount of information, and the amount of information transmitted from the roof cover to the undercarriage foundation is much greater than that transmitted from the roof cover to the generator floor slab.

The TE value change curve of vibration test condition 3 (the moment when the hydropower station unit is shut down) is shown in Fig. 10.

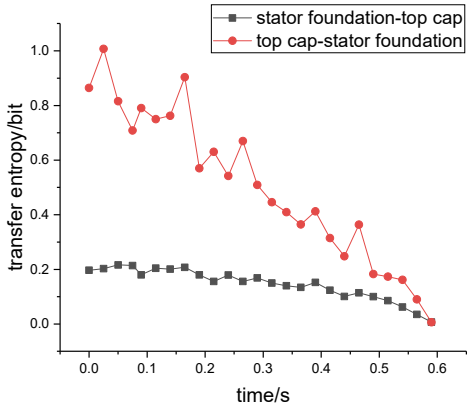

(a) TE curve of the stator base and the roof cover

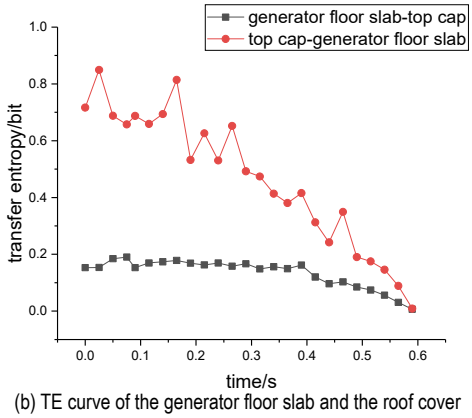

(b) TE curve of the generator floor slab and the roof cover

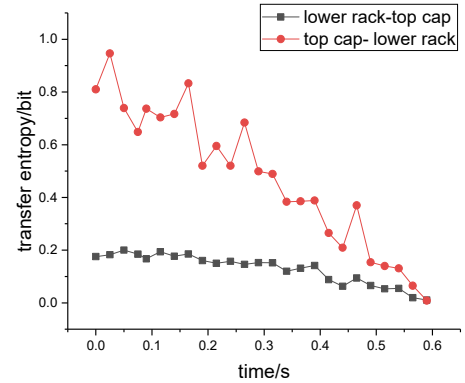

(c) TE curve of the undercarriage and the roof cover

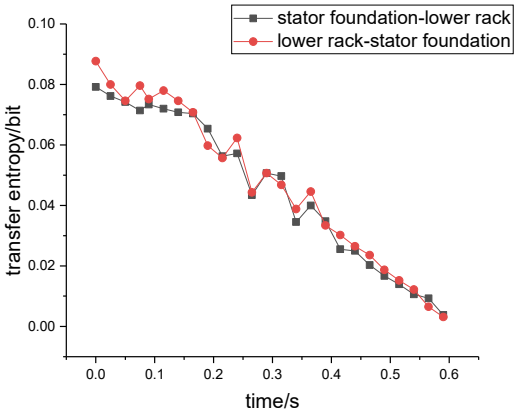

(d) TE curve of the generator floor slab and the stator base

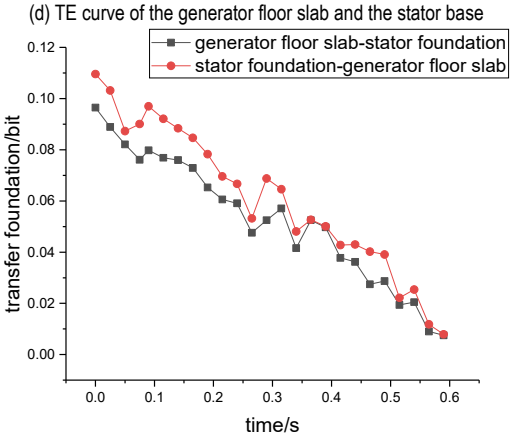

(e) TE curve of the undercarriage and stator base

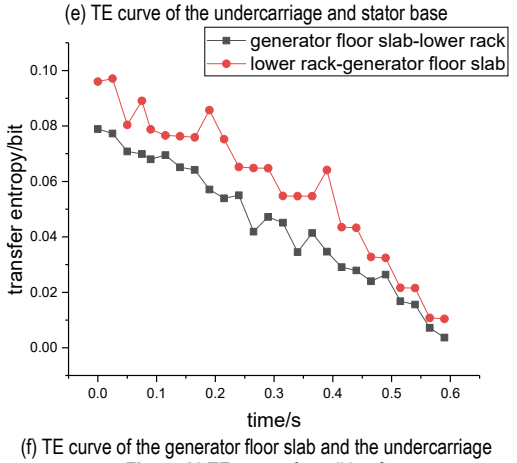

(f) TE curve of the generator floor slab and the undercarriage

Figure 10 TE curve of condition 3

The TE value represents the degree of correlation between two signals. When the hydroelectric generating unit of a hydropower station starts to shut down (test condition 3), the TE value is lower than that at the same measurement point in a stable operating state. Moreover, as the hydroelectric generating unit is shut down, the TE value shows a decreasing trend with the shutdown time, which is consistent with the actual operating state. Fig. 10 indicates that the correlation degree between the two measurement points is gradually weakening at the time of shutdown until the TE reaches 0.

By comparing and analyzing Figs. 8, 9 and 10, it can be obtained that: (1) under different working conditions of the hydroelectric generating unit, the entropy value of the vortex rope of vibration signal transmission between the measurement points will change, but the transfer path does not change significantly. (2) Based on the magnitude distribution of TE values among different working conditions and measurement points, the vibration signal transmission law can be analyzed as follows. Roof cover $\rightarrow$ undercarriage $\rightarrow$ Generator floor slab and Roof cover $\rightarrow$ Stator $\rightarrow$ Generator floor slab (3) When the unit operates smoothly, the entropy value of the TE is relatively large, the vibration energy of the vortex rope is strong, and the correlation degree between the measurement points is high. Now when the unit is turned on or off, the entropy value of the TE significantly decreases, indicating that there is less information transmission between the measurement points and the vibration signal of the vortex rope is weak. Analyzing the reason, it may be that now when the unit is turned on or off, the water flow has not yet completely passed through the hydroelectric generating unit, and the CEEMDAN-SVD algorithm is introduced to filter out the vibration signals of the mechanical and electromagnetic parts. Therefore, the weak vibration signal of the vortex rope leads to less transmission of water flow vibration signals between measurement points.

Among the hydraulic vibration sources, the roof cover to a certain extent represents the vibration condition of the vortex rope in the draft tube. The vibration of the vortex rope is transmitted from the bottom of the wind hood to the machine pier, and then from the machine pier to the generator floor slab. Therefore, the transfer path of the vibration signal in the vortex rope is analyzed as follows, vertex rope $\rightarrow$ Frame pier $\rightarrow$ generator floor slab :

4.4 Information Transmission Rate

To quantitatively verify the effectiveness of the combination of CEEMDAN-SVD and TE, the Information Transfer Raite (ITR for short) is introduced. ITR quantitatively describes the ratio of energy to information, which is an important indicator of the characteristics of information transmission channels. The information transmission rate ITR of a random process is x and y.

$$ITR_{y\to x}=\frac{T_{y\to x}-T_{x\to y}}{T_{y\to y}}\in[0,1] \tag{15}$$

In the formula, $\mathrm{ITR}_{\mathrm{y\to x}}$ represents the information transmission rate of $y\to x$, $T_{y\to x}$ and $T_{x\to y}$ are the TE values of x, y respectively. $T_{y\to y}$ transmits all the information of y to x. $\left(T_{y\to x}-T_{x\to y}\right)$ is the net transmission quantity of the signal $y\to x$. When $\mathrm{ITR}_{\mathrm{y\to x}}=0$ is present, signals x and y do not transmit any information, and the two signals are independent signals. When $\mathrm{ITR}_{\mathrm{y\to x}}=1$ indicates that all the information of y is transmitted to x, in an ideal state, the signal can be transmitted completely without loss. Generally speaking, $\mathrm{ITR}_{y\to x}\neq\mathrm{ITR}_{x\to y}$.

To quantitatively verify the information transmission process of the vibration signal caused by the vortex tope in the structure of the hydropower station building, the information transmission rate between the measurement

points was calculated, as shown in Tabs. 2, 3 and 4.

Table 2 Information transmission rate when the hydroelectric generating unit of the hydropower station is turned on (Test Condition 1)

Measurement point	top cap→stator foundation	stator foundation→top cap	top cap→lower rack	lower rack→generator floor slab
Information transmission rate %	4.5	6.8	17.2	9.73

Table 3 Information transmission rate of hydroelectric generating units in hydropower stations during Stable operation (Test Condition 2)

Measurement point	top cap→stator foundation	stator foundation→top cap	top cap→lower rack	lower rack→generator floor slab
Information transmission rate %	37.8	21.5	45.2	24.3

Table 4 Information transmission rate when the hydroelectric generating unit of a hydropower station starts to shut down (Test Condition 3)

Measurement point	top cap→stator foundation	stator foundation→top cap	top cap→lower rack	lower rack→generator floor slab
Information transmission rate %	12	4.7	14.3	6.2

By calculating the information transmission rate between signals, the correctness of the method based on the combination of CEEMDAN-SVD and TE for the analysis and identification of vibration transfer paths in hydropower station plants was quantitatively verified. By comparing the TE and ITR at each measurement point, it can be concluded that under test condition 2 (stable operation of the hydroelectric generating unit), $ITR_{\text{roof cover}\rightarrow\text{Stator base}} = 37.8\%$ and $ITR_{\text{roof cover}\rightarrow\text{undercarriage}} = 45.2\%$. A larger portion of the energy from the roof cover is transferred to the stator and the foundation of the undercarriage. The transfer rate from the roof cover to the undercarriage may be higher, but overall, the transfer paths of the two paths are not very high, which may be related to the energy dissipation and vibration prevention of the factory building structure. $ITR_{\text{undercarriage}\rightarrow\text{generator floor slab}} = 24.3\%$ and $ITR_{\text{stator base}\rightarrow\text{generator floor slab}} = 21.5\%$. The transmission rate from the machine pier to the generator floor slab is relatively low. These observations reveal two complementary features: first, only a modest amount of signal is being transmitted, and second, both the under-carriage and the stator base intrinsically carry low vibrational energy. The consistency between the measured transfer-entropy values and the expected energy distribution confirms the reliability of the TE-based transmission analysis. In addition, when the generating units are running under off-design or unsteady conditions the information-transfer rate between measurement points drops markedly. At these moments, the flow has not fully engaged the runner, so the vortex rope produces only weak vibration energy that is poorly propagated through the structure. Conversely, during stable operation the decline in transmission rate is primarily attributable to the power house concrete itself: its mass and internal damping dissipate a measurable fraction of the vibrational energy, attenuating the signal as it travels through the block and footings.

Energy dissipation primarily refers to converting external loads (e.g., earthquakes, wind-induced vibrations, mechanical vibrations) into heat or other forms of energy through structural designs or auxiliary devices, thereby reducing damage to the main structure. This requires a systematic approach combining source control (isolating vibration sources), path interruption (vibration isolation measures), and structural reinforcement (energy dissipation design). By strategically selecting dampers, seismic isolation technologies, dynamic frequency modulation devices, and intelligent monitoring systems, the safety and adaptability of industrial facilities under dynamic loads can be significantly enhanced.

5 CONCLUSION

To enhance the accuracy and representativeness of vibration transmission analysis, this paper proposes a vibration transfer path analysis method for the power house of hydroelectric power stations combining CEEMDAN-SVD and TE. The effectiveness of the algorithm is verified through simulation signals. Taking the observation signals of the real power house of a hydroelectric power station prototype as the object, the vibration transfer path caused by the vortex rope is analyzed. The following conclusions are drawn:

Two sets of vibration simulation signals were constructed. Through calculation and comparison, it can be determined that the TE algorithm accurately determines the transmission law between the signals, which reflects the correlation between the two signals, and exhibits certain anti-noise performance, verifying that the TE algorithm is suitable for the analyzing of the transmission law of vibration signals.

(2) Based on the combined algorithm of CEEMDAN-SVD and TE, the vibration measurement data were preprocessed to separate the vibration signals caused by the vortex rope, and the transfer path was analyzed. It was obtained that the transfer path of the vortex rope vibration in the power house of hydroelectric power station structure under different working conditions is as follows: draft tube → undercarriage foundation, stator base → generator floor slab.

(3) ITR is introduced to quantitatively evaluate the effectiveness of the methods. By comparing the TE, ITR, and actual operational conditions at each measurement point, it is verified that the combined CEEMDAN-SVD and TE method demonstrates strong applicability and effectiveness in analyzing vibration information transmission within the power house of a hydropower station. These findings provide a scientific basis for vibration control and structural health monitoring in hydraulic engineering, and offer new insights for damage detection and diagnosis.

(4) Through both qualitative and quantitative indicators, the analysis reveals that during the transmission process of vortex rope vibration signals within the power house structure, the concrete structure absorbs a portion of the vibrational energy. This suggests that further investigation into the relationship between structural material composition and vibration transmission paths could contribute to more effective vibration control strategies for engineering structures.

Acknowledgments

The research was supported by General Project of Henan Provincial Natural Science Foundation (242300420041), the key scientific and technological projects in Henan Province (252102320031), the Key scientific research project plan of Henan Higher Education Institutions (23A570010) and Kaifeng science and technology project (2303003, 2303058, 2403102).

6 REFERENCES

[1] Zhang, Y. C. (2021). *Study on vibration transfer of pumped storage power plant based on energy method*. Doctoral dissertation, Dalian University of Technology.

[2] Shi, L. J. (2022). *Study on the transmission path of vibration to the main plant based on the structural sound intensity method for water relief buildings*. Doctoral dissertation, Dalian University of Technology.

[3] Wang, H. J., Tu, K., & Li, J. J. (2012). Experimental study on grouting bleed of compound cross-section aperture for post-tensioning structure. *Journal of Hydraulic Engineering*, *43*(5), 615-622.

[4] Xu, W., Ma, Z. Y., & Zhi, B. P. (2012). Analysis on frequency response to pulsating pressure in large hydro-power house based on the theory of power flow. *Journal of Hydraulic Engineering*, *43*(5), 615-622.

[5] Qin, L. (2005). *Dynamic analysis and identification of powerhouse structure of two-row placed units*. Doctoral dissertation, Tianjin University.

[6] Lindner, B., Auret, L., Bauer, M., & Groenewald, J. W. (2019). Comparative analysis of Granger causality and TE to present a decision flow for the application of oscillation diagnosis. *Journal of Process Control*, *79*, 72-84. https://doi.org/10.1016/j.jprocont.2019.03.009

[7] Gao, X. F. (2023). *Study on contact behavior and vibration transmission on the interface between steel spiral case and surrounding concrete in pumped storage power plants*. Doctoral dissertation, Wuhan University.

[8] Wei, P. (2022). *Sensitivity analysis and vibration characteristics of shaft system parameters of hydro-generator set*. Doctoral dissertation, Xian University of Technology.

[9] Kaiser, A. (2002). Information transfer in continuous processes. *Physica D: Nonlinear Phenomena*, *166*(1/2), 43-62. https://doi.org/10.1016/S0167-2789(02)00644-7

[10] Mousavi, A. A., Zhang, C., Masri, S. F., & Gholipour, G. (2022). Structural damage detection method based on the complete ensemble empirical mode decomposition with adaptive noise: A model steel truss bridge case study. *Structural Health Monitoring*, *21*, 887-912. https://doi.org/10.1177/14759217211012787

[11] Schreiber, T. (2000). Measuring information transfer. *Physical Review Letters*, *85*(2), 461-464. https://doi.org/10.1103/PhysRevLett.85.461

[12] Nichols, J. M. (2005). Detecting non-linearity in structural systems using the TE. *Physical Review E*, *72*(4), 1-11. https://doi.org/10.1103/PhysRevE.72.046207

[13] Nichols, J. M. (2006). Examining structural dynamics using information flow. *Probabilistic Engineering Mechanics*, *21*(4), 420-433. https://doi.org/10.1016/j.probengmech.2005.09.002

[14] Overbey, L. A. (2009). Dynamic system change detection using a modification of the TE. *Journal of Sound and Vibration*, *32*(1-2), 438-453. https://doi.org/10.1016/j.jsv.2008.07.037

[15] Cheng, M. R. (2021). *Quxue research on vibration monitoring of hydro-power plant building*. Doctoral dissertation, North China University of Water Resources and Electric Power.

[16] Zhang, J. W., Hou, G., & Bao, Z. L. (2017). A signal de-noising method for vibration signals from flood discharge structures based on CEEMDAN and SVD. *Journal of Vibration and Shock*, *36*(22), 138-143.

Contact information:

Baoping ZHI
1) Huge Water Network Disaster Prevention Engineering Technology Research Center of Henan Province, Kaifeng 475004, China
2) Henan Province Engineering Research Center of Operation and Ecological Safety of Inter Basin Region Water Diversion Projects in Inter Basin Areas, Kaifeng, 475004, China
3) Yellow River Conservancy Technical University, Kaifeng, 475004, China

Mengran CHENG
1) Huge Water Network Disaster Prevention Engineering Technology Research Center of Henan Province, Kaifeng 475004, China
2) Yellow River Conservancy Technical University, Kaifeng, 475004, China

Jingjing QIN
(Corresponding author)
1) Huge Water Network Disaster Prevention Engineering Technology Research Center of Henan Province, Kaifeng 475004, China
2) Yellow River Conservancy Technical University, Kaifeng, 475004, China
E-mail: zbphx2025@163.com

Zihan SONG
Yellow River Conservancy Technical University,
Kaifeng, 475004, China